THE JOURNAL OF BIOLOGICAL CHEMISTRY
Vol. 278, No. 33, Issue of August 15, pp. 31192–31201, 2003

Printed in U.S.A.

Studies on the Internalization Mechanism of Cationic Cell-penetrating Peptides*

Received for publication, April 15, 2003, and in revised form, May 23, 2003
Published, JBC Papers in Press, June 3, 2003, DOI 10.1074/jbc.M303938200

Guillaume Drin‡§, Sylvine Cottin‡§, Emmanuelle Blanc‡, Anthony R. Rees¶, and Jamal Temsamani¶‖

From the ‡Synt:em, Institut de Génétique Moléculaire, 1919 Route de Mende, 34293 Montpellier Cedex 5, France and ¶Synt:em, Parc Scientifique Georges Besse, 30000 Nîmes, France

A great deal of data has been amassed suggesting that cationic peptides are able to translocate into eucaryotic cells in a temperature-independent manner. Although such peptides are widely used to promote the intracellular delivery of bioactive molecules, the mechanism by which this cell-penetrating activity occurs still remains unclear. Here, we present an *in vitro* study of the cellular uptake of peptides, originally deriving from protegrin (the SynB peptide vectors), that have also been shown to enhance the transport of drugs across the blood-brain barrier. In parallel, we have examined the internalization process of two lipid-interacting peptides, SynB5 and pAntp-(43–58), the latter corresponding to the translocating segment of the Antennapedia homeodomain. We report a quantitative study of the time- and dose-dependence of internalization and demonstrate that these peptides accumulate inside vesicular structures. Furthermore, we have examined the role of endocytotic pathways in this process using a variety of metabolic and endocytosis inhibitors. We show that the internalization of these peptides is a temperature- and energy-dependent process and that endosomal transport is a key component of the mechanism. Altogether, our results suggest that SynB and pAntp-(43–58) peptides penetrate into cells by an adsorptive-mediated endocytosis process rather than temperature-independent translocation.

A large number of hydrophilic molecules such as peptides, proteins, and oligonucleotides are poorly internalized by cells because they cross the lipid matrix of the plasma membrane rather inefficiently. This is considered to be a major limitation for their use as therapeutic agents in biomedical research and the pharmaceutical industry. However, it has been reported that the use of short (10–30 amino acids) cationic peptides may provide a solution by enhancing the intracellular delivery of such intractable molecules, both *in vitro* and *in vivo* (see reviews in Refs. 1–3).

These cell-penetrating peptides (CPPs)[1] are either basic segments of RNA- or DNA-binding proteins (4, 5, 6) such as pAntp-(43–58) and Tat-(48–60), or artificial peptides such as Transportan (7), model amphipathic peptide (MAP) (8), or other sequence-based constructs (9, 10). In addition, the SynB peptides constitute a distinct family of vectors that derive from protegrin 1 (PG-1), an antimicrobial peptide (11). As reported previously, PG-1, the amphipathic structure of which is stabilized by two disulfide bridges (12), is believed to exert its antibiotic action by forming pores in the lipid matrix of bacterial membranes (13, 14). Because it has been shown that this pore formation depends critically on a cyclic, disulfide-bonded structure (13), we designed two analogs, SynB1 and SynB3, that lack the cysteine residues. We then investigated whether these linear peptides, which possess the multiple positive charges of PG-1, were able to penetrate into eukaryotic cells without disrupting the cell membrane. This was shown to be the case, with SynB1 and SynB3 efficiently promoting the transport of various drugs such as doxorubicin and benzylpenicillin (15, 16) across the blood-brain barrier of *in vivo* models. An unexpected benefit of the "vectorization" of the PG-p substrate doxorubicin was that its accumulation and potency in resistant K562 cells was improved drastically (17).

Understanding the mode of entry of the SynB peptides and defining their intracellular localization are of particular interest for the design of conjugates which, once internalized in target cells, may efficiently release an attached drug in its native state. Several previous studies have proposed that the penetration of CPPs (such as pAntp-(43–58), Tat-(48–60), MAP, and Transportan) into eukaryotic cells occurs in a temperature-independent manner (4, 5, 7, 8). Furthermore, by using various metabolic or endocytosis inhibitors, it has been suggested that the cell-penetrating ability of some CPPs is likely to be an energy-independent, non-endocytotic process (5, 7, 18). Additional studies showed that the cell penetration of enantio or inverso forms of peptides such as MAP or pAntp-(43–58) was as efficient as that of the parent peptides (8, 19, 20), suggesting that their internalization is not dependent on a chiral receptor.

To explain these observations, it has been mainly proposed that the hydrophobicity and amphipathicity of CPPs confers on them the ability to interact with and pass through the lipid matrix of the plasma membrane via an energy-independent process termed translocation (1, 7, 20). In accord with this model, biophysical studies have indicated that pAntp-(43–58), Transportan, or MAP can interact with lipid vesicles while adopting a helical structure (21–24). Furthermore, based on several reports indicating that amphipathic anti-microbial and

* The costs of publication of this article were defrayed in part by the payment of page charges. This article must therefore be hereby marked "*advertisement*" in accordance with 18 U.S.C. Section 1734 solely to indicate this fact.

§ These authors contributed equally to this work.
‖ To whom correspondence should be addressed. Tel.: 33-466-048666; Fax: 33-466-048667; E-mail: jtemsamani@syntem.com.

[1] The abbreviations used are: CPP, cell-penetrating peptide; calcein-AM, calcein acetoxymethylester; CoxIV, cytochrome oxidase IV mitochondrial import (peptide/presequence); FITC, fluorescein isothiocyanate; Fmoc, *N*-(9-fluorenyl)methoxycarbonyl; LY, Lucifer Yellow CH; MAP, model amphipathic peptide; NBD, 4-chloro-7-nitrobenz-2-oxa-1,3-diazole; NEM, *N*-ethylmaleimide; PBS, phosphate-buffered saline; PG-1, protegrin 1; POPC, 1-palmitoyl-2-oleyl-*sn*-glycero-3-phosphocholine; POPG, 1-palmitoyl-2-oleyl-*sn*-glycero-3-phosphoglycerol; TAMRA, 5-(and-6)-carboxytetramethylrhodamine; Tf, transferrin.

venom peptides are able to cross lipid bilayers (see review in Ref. 25), we measured the ability of pAntp-(43–58) to pass from the outer to the inner leaflet of a phospholipid membrane. However, our data revealed an absence of spontaneous translocation despite the lipid-binding ability of this CPP (26). In a similar biophysical study, we demonstrate that PG-1 is able to cross the membrane of phospholipidic vesicles but that a linear analogue, SynB5, is not able to do this despite having a similar lipid-binding activity. This suggested, and was subsequently borne out, that similar linear vectors may also lack the translocation property of the protegrins (27). Having said that, artificial phospholipid bilayers may not be an ideal, realistic experimental model in which to investigate CPP passage across the plasma membrane. Therefore, it seemed important to directly examine in cells whether the uptake of diverse SynB peptides was related to the translocation mechanism described for others CPPs or depended on a metabolic cellular process.

In this study, we examine the cell uptake of the SynB1 and SynB3 peptides (Table I) compared with that of pAntp-(43–58). We also examine the internalization of SynB5, for which we have also measured its translocation activity in lipid vesicles (27). Because these four cationic peptides differ in terms of hydrophobicity and/or helical amphipathicity (Table I), this study could also indicate whether their individual physicochemical properties conferred on them specific mechanistic preferences.

We have measured time- and dose-dependence of the CPPs uptake into K562 cells and examined the influence of various metabolic and endocytosis inhibitors on the internalization. We have also carried out complementary experiments to measure the diffusion of pAntp-(43–58) through a lipid bilayer and examined the effect of cell fixation on the intracellular localization of CPPs. Our results indicate that SynB and pAntp-(43–58) peptides penetrate into cells via an adsorptive-mediated endocytosis process rather than a temperature-independent translocation mechanism.

EXPERIMENTAL PROCEDURES

Materials—Fmoc-PAL-PEG-PS (High Load) and Fmoc amino acids were purchased from Perseptive Biosystems (Hamburg, Germany). Other reagents used for peptide synthesis included *N*,*N*′-diisopropylcarbodiimide (DIPCDI, Fluka), 1-hydroxybenzotriazole (HOBT, PerkinElmer Life Sciences), *N*,*N*-diisopropylethylamine (DIEA, Fluka), dimethylformamide (DMF, Perseptive Biosystems), 4-chloro-7-nitrobenz-2-oxa-1,3-diazol-4-yl (NBD-Cl, Fluka), and 5-(and-6)-carboxytetramethylrhodamine (TAMRA; Molecular Probes, Eugene, OR). Sodium dithionite, sodium azide, *N*-ethylmaleimide, 2-deoxy-D-glucose, vinblastine, nocodazole, cytochalasin D, bafilomycin A1, chloroquine, nystatin, digitonin, Lucifer Yellow (LY), poly-L-lysine, valinomycin, Triton X-100, and trypsin were supplied by Sigma. Calcein-AM, FITC-transferrin (Tf), Texas Red-Tf, and DiSC3 (5) were purchased from Molecular Probes. Reagents for cell biology including Opti-MEM, RPMI 1640, and fetal bovine serum were obtained from Invitrogen. The lipids 1-palmitoyl-2-oleyl-*sn*-glycero-3-phosphocholine (POPC) and 1-palmitoyl-2-oleyl-*sn*-glycero-3-phosphoglycerol (POPG) were obtained from Avanti Polar Lipids (Alabaster, AL).

Peptide Synthesis and Fluorescent Labeling—All peptides were synthesized according to the Fmoc-*tert*-butyl strategy using an AMS 422 multiple peptide synthesizer (Abimed, Langenfeld, Germany). Labeling of the N terminus of peptides with the NBD or TAMRA probe was achieved as follow. Briefly, resin-bound peptide was treated with piperidine (20% (v/v) in dimethylformamide) in order to remove the N-terminal Fmoc protecting group. NBD-Cl or TAMRA was added in dry dimethylformamide (5-fold molar excess) in the presence of diisopropylethylamine (DIEA; 2-fold molar excess) for 6 h under agitation in the dark to selectively label the N-terminal amino group. The resin was washed with dimethylformamide and treated with deprotecting mixture to cleave the peptides from the resin and deprotect the side chains. For labeling the CoxIV peptide, the deprotected peptide was *S*-alkylated with *N*,*N*′-dimethyl-*N*-(iodoacetyl)-*N*′-(7-nitrobenz-2-oxa-1,3-diazol-4-yl) ethylene-diamine (IANBD) amide (Molecular Probes) on cysteine residues in dimethylformamide. Peptide purification was carried out by reverse phase high pressure liquid chromatography (Water-prep LC 40, Waters) using a 0.01% trifluoroacetic acid/acetonitrile gradient. Purity, as assessed by reverse phase analytic chromatography (Beckman Gold equipped with a diode array detector), was >95% for all peptides by the criterion of relative UV absorbencies at 220 nm and at either 460 (for NBD-labeled peptides) or 540 nm (for TAMRA-labeled peptides). The molecular masses were validated by matrix-assisted laser desorption/ionization-time of flight mass spectroscopy (MALDI-TOF MS; Voyager Elite, Perseptive Biosystems). The peptide concentration of unlabeled peptide was determined by absorption spectroscopy, considering the extinction coefficient of tryptophan, tyrosine, and phenylalanine equal to 5680, 1270, and 260 M^{-1} cm^{-1}, respectively, at 280 nm. For NBD- and TAMRA-labeled peptides, the extinction coefficients provided by the probe manufacturer were used.

Cell Culture—K562 cells were purchased from the American Type Culture Collection and cultured in RPMI 1640 supplemented with 10% (v/v) calf serum (Invitrogen) without antibiotics. Cells were grown on 100-mm dishes in an atmosphere of 5% CO_2 at 37 °C.

Quantification of Internalized NBD-labeled Peptides—K562 cells were diluted to 3×10^5 cells·ml^{-1} in culture medium 1 day before the experiment. Cell association and internalization of peptides were measured by flow cytometry using a FACSCaliber (BD Biosciences) driven by the CellQuest software. The flow cytometer was periodically calibrated using fluorescent beads (Calibrite3, BD Biosciences). The day of the experiment the cells were counted, centrifuged, and resuspended in pre-warmed Opti-MEM (37 °C) to obtain a suspension at 6×10^5 cells·ml^{-1}. After a 1-h incubation, the NBD-labeled peptides were incubated with K562 cells in the same medium at 37 °C (final volume was 0.5 ml). Thereafter, the cells were washed twice and resuspended in 0.5 ml (final volume) of ice-cold PBS for flow cytometry analysis. Cell-associated fluorophores were excited at 488 nm, and fluorescence was measured at 525 nm. A cytogram (1×10^4 counts) was acquired, and the cells exhibiting a normal morphology (~95% of the total, unless otherwise specified) were taken into account to obtain a histogram of fluorescence intensity per cell. The calculated mean of this distribution was considered as representative of the amount of cell-associated peptides. A stock solution of dithionite (1 M) was freshly prepared in 1 M Tris solution (pH 10). Following flow cytometry analysis, 5 μl of dithionite stock solution was added to cells maintained at 4 °C, and the fluorescence of internalized peptides was measured after 5 min.

Peptide and Endocytosis Marker Visualization—TAMRA-labeled peptides (1–3 μM) were incubated with K562 cells in an Opti-MEM medium at 37 °C for 90 min. Thereafter, the cells were washed twice with ice-cold PBS and resuspended in 20 μl (final volume) in the same buffer. Suspensions were plated on glass slides and observed immediately without fixation. For visualizing the intracellular localization of Tf or LY, the cells were incubated with either Texas Red-Tf (incubated for 30 min at 25 μg·ml^{-1}) or LY (90 min at 1 mg·ml^{-1}), washed with ice-cold PBS, plated on poly-L-lysine-coated slides for 45 min, fixed with 3.7% formaldehyde (Sigma) in PBS for 10 min, washed, and mounted with PermaFluor® (CML). Confocal images were obtained with a DMR-B Leica microscope equipped with a argon-krypton ion laser with the excitation line at 488 nm or 568 nm (the emission filter was at 525 and 600 nm, respectively) and fitted with a PerkinElmer Ultraview module (PerkinElmer Life Sciences). The samples were observed with a 100× oil immersion PL AZO HCX lens. The images were captured with a CoolSnap HQ camera (Photometrics) at 696 × 520 pixel resolution. The whole set was controlled with the MetaMorph software (Universal Imaging Corporation).

Quantification of Receptor-mediated and Fluid Phase Endocytosis—K562 cells were incubated in Opti-MEM at 37 °C with FITC-Tf (25 μg·ml^{-1}) for 30 min or LY (1 mg·ml^{-1}) for 90 min at 37 °C in Opti-MEM. The uptake was stopped by washing the cells twice with ice-cold PBS (the final volume was 0.5 ml). Cell-associated fluorophores were excited at 488 nm, and fluorescence was measured at 525 nm. A histogram was generated, and the calculated mean of the distribution of fluorescence intensity per cell (10^4 counts) was considered as representative of the amount of markers associated with the cells.

Calcein-AM Release Assay—The cells were incubated with 2.5 μM calcein-AM for 60 min in Opti-MEM, washed, resuspended in the same volume of calcein-free Opti-MEM, and incubated with peptide for 90 min at 37 °C. The cells were washed once with ice-cold PBS, and the calcein content of cells was determined by flow cytometry. Digitonin (100 μg·ml^{-1}) induced the complete lysis of K562 cells after an incubation of 90 min. The apparent percent leakage value was calculated according to the equation $100 \times (F - F_0)/(F_{max} - F_0)$. F_0 and F_{max} correspond to the mean fluorescence intensity associated with normal cells and digitonin-treated cells, respectively. F represents the fluorescence of the calcein-loaded cells incubated with the peptides.

TABLE I
Name, sequence and physicochemical features of cell-penetrating peptides

Peptide	Sequence[a]	Length	Net Charge	$\langle H \rangle^b$	$\langle \mu H \rangle^b$
SynB1	**R**GG**R**LSYS**RRR**FSTSTG**R**	18	6	−0.1	0.158
SynB3	**RR**LSYS**RRR**F	10	5	−0.124	0.361
SynB5	**R**GG**R**LAYL**RRR**WAVLG**R**	18	6	0.238	0.213
pAntp-(43–58)	**RQIK**IWFQN**RR**M**K**W**KK**	16	7	0.193	0.33

[a] The basic residues are indicated in boldfaced type.
[b] The mean hydrophobicity H and mean helical hydrophobic moment μH of each peptide was calculated following the Eisenberg formula (31) with the hydrophobic scale of Fauchère and Pliska, based on the octanol/water partition of individual N-acetyl amino acid residues (32).

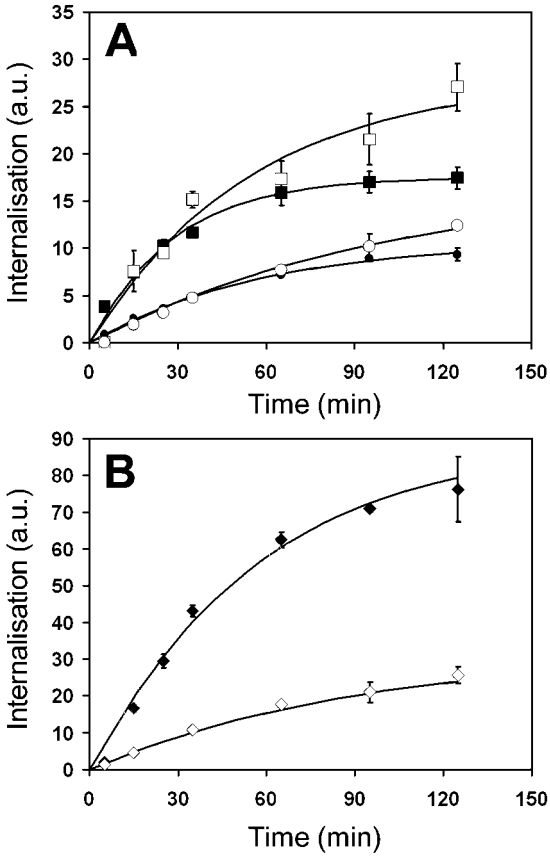

FIG. 1. **Kinetic of uptake of SynB and pAntp-(43–58) peptides in K562 cells.** *A* and *B*, K562 cells (6×10^5 cells·ml^{-1}) were incubated with NBD-labeled peptides at 6 μM (except SynB5 and pAntp-(43–58), which were incubated at 3 and 1 μM, respectively) in Opti-MEM for various incubation times at 37 °C. The amount of internalized peptide was determined by the NBD/dithionite assay (see "Experimental Procedures"). Each point is the mean ± S.D. of three separate determinations. For each point, the mean fluorescence intensity measured with the cells alone was subtracted from the mean fluorescence intensity measured with the peptide. ●, SynB1; ○, D-SynB1; ■, SynB3; □, D-SynB3; ♦, SynB5; and ◇, pAntp-(43–58). *a.u.*, arbitrary units.

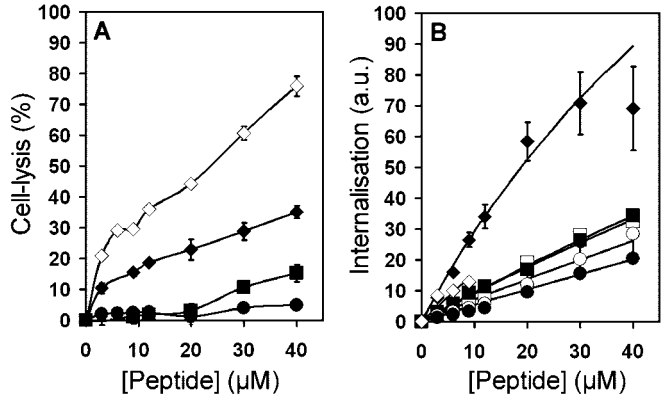

FIG. 2. **Dose dependence of the cell lysis and uptake of SynB and pAntp-(43–58) peptides.** *A*, calcein-loaded K562 cells (6×10^5 cells·ml^{-1}) were incubated with various concentration of unlabeled peptide for 90 min at 37 °C in Opti-MEM. The cells were washed once with ice-cold PBS, and the calcein content of cells was determined by flow cytometry. The percentage of cell lysis was calculated as described under "Experimental Procedures." Each point is the mean ± S.D. of three separate determinations. ●, SynB1; ■, SynB3; ◇, SynB5; and ♦, pAntp-(43–58). *B*, K562 cells (6×10^5 cells·ml^{-1}) were incubated for 15 min at 37 °C in Opti-MEM with increasing concentrations of NBD-labeled peptides. Peptide internalization was determined using the NBD/dithionite assay (see "Experimental Procedures"). For SynB5 and pAntp-(43–58) peptides, only a viable subpopulation of cells (~70% of the total population) was taken into account to calculate the mean fluorescence intensity at each peptide concentration. Each point is the mean ± S.D. of three separate determinations. For each point, the fluorescence intensity measured with the cells alone was subtracted from the mean fluorescence measured with the peptide. ●, SynB1; ○, D-SynB1; ■, SynB3; □, D-SynB3; ◇, SynB5; and ♦, pAntp-(43–58). *a.u.*, arbitrary units.

Metabolic and Endocytosis Inhibitor Studies—For experiments at a low temperature, the cells were maintained for 30 min on ice before peptide incubation and throughout the experiment. To induce ATP depletion, the cells were incubated for 60 min with 0.1% sodium azide and 50 mM 2-deoxy-D-glucose (DOG) in Opti-MEM prior to the addition of peptide. The ATP cellular concentration was determined using the bioluminescent assay kit from Sigma according to the manufacturer's instructions. The luminescent signal was measured in a 96-well plate with a Tecan Spectrafluor reader. The inhibition of microtubule polymerization was induced by treating cells with vinblastine or nocodazole at 10 μM or 20 μM, respectively, 1 h prior to the addition of peptide. Cytochalasin D was added at 10 μM for 1 h prior to the addition of peptide to block actin polymerization. For NEM treatment, cells were exposed to NEM (10 μM) in Opti-MEM for 5 min and then washed in a NEM-free medium containing the peptide. The neutralization of pH in intracellular acidic compartments was achieved by pre-incubating cells with 10 mM NH_4CL for 10 min or with 50 μM chloroquine or 200 nM bafilomycin A1 for 30 min before peptide addition. For the nystatin treatment, cells were exposed to the reagent at 25 μg·ml^{-1} for 30 min before the addition of the peptide. Inhibition assays with poly-L-lysine were performed by incubating the peptide for 15 min with cells in the absence or presence of the compound (300 μM). Prior to these experiments, we made sure that the various inhibitors were used at a concentration that maintained the plasma membrane integrity by performing a calcein-AM assay.

Measure of Peptide Translocation in Lipidic Vesicles—Large unilamellar vesicles were prepared by drying a lipid film of POPC and POPG (at a 3:1 molar ratio) for 3 h and then resuspending the lipids in buffer (20 mM Tris and 100 mM KCl, pH 7). The lipid suspension was freeze-thawed for five cycles and then extruded through polycarbonate filters (0.1-μm pore size) 21 times. Valinomycin (22.5 μM in ethanol) was added to the large unilamellar vesicles at a lipid-to-valinomycin molar ratio of ~10,000. The lipid concentration was determined in duplicate by phosphorus analysis as described previously (28). Fluorescence measurements were performed in 3-ml quartz cells at 25 ± 0.1 °C under constant magnetic stirring using a SLM AB-2 spectrofluorometer (SLM Instruments, Inc., Urbana, IL). For measuring the NBD-labeled peptide translocation, excitation and emission wavelengths were set at 460–485 nm and 530–540 nm, respectively. Excitation and emission band pass values were set at 4 nm for both cases. In the translocation assays, the membrane potential was generated by diluting 100-fold valinomycin-containing vesicles in KCl-free buffer (20 mM Tris and 100 mM NaCl, pH 7). The presence of the negative potential was assessed in a separate assay by measuring the fluorescence of DiSC3 (5) probes (λ_{ex} = 622 nm; λ_{em} = 670 nm) as described previously (29).

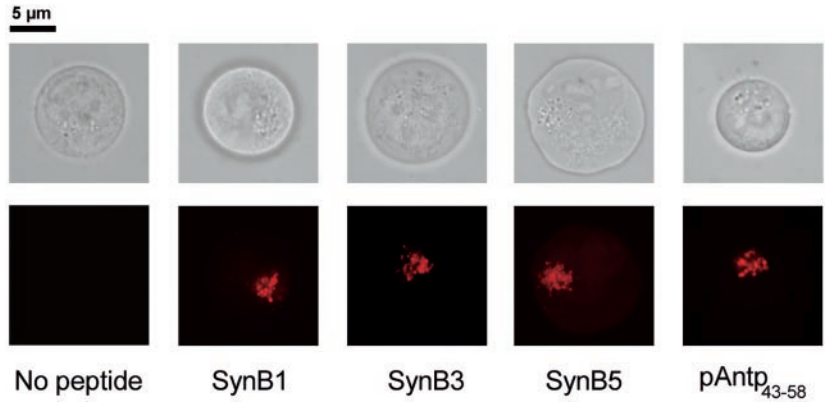

FIG. 3. **Localization of cell-penetrating peptides in K562 cells.** K562 cells (6×10^5 cells·ml^{-1}) were incubated with TAMRA-labeled peptides either at 3 μM (SynB1 and SynB3) or 1 μM (SynB5 and pAntp-(43–58)) in Opti-MEM for 90 min. Cells were then washed carefully twice with ice-cold PBS (final volume of 50 μl) and immediately observed by confocal fluorescence microscopy. Cells were incubated without peptide as control. The optical sections presented were taken approximately at the mid-height level of cells. Photos obtained by light microscopy show the contour of cells.

RESULTS

Time Course—In previously published studies, we have described a method based on the chemical quenching of the NBD fluorophore by the membrane-impermeant dithionite, allowing direct measurement of the amount of internalized NBD-labeled peptide (30). To obtain information about the time course of the internalization of the SynB peptides and the pAntp-(43–58) peptide (Table I), we have applied the NBD/dithionite assay to K562 cells incubated with each NBD-labeled peptide for different incubation times (from 0 to 120 min). As shown in Fig. 1, *A* and *B*, the cell uptake of the SynB and pAntp-(43–58) peptides takes place in the first minutes and reaches a maximum after ~1 h. Fig. 1*A* also demonstrates that the D-amino acid analogs of SynB1 and SynB3 penetrate into cells as efficiently as their L-amino acid counterparts for the first hour. Furthermore, it can be seen that, over the 2-h period of exposure, the cumulative amounts of internalized D-SynB1 and D-SynB3 were higher than those of the L-counterparts. We believe this may arise from retention of the D-peptides within the endosome compartment, partly due to their resistance to proteolysis.

Concentration Dependence of Peptide Internalization and Cell Lytic Activity—The dependence of the initial rate of cellular uptake on peptide concentration (0–40 μM) was examined in K562 cells over a period of 15 min. To control for cell integrity, we used a calcein-AM retention assay in which we observed that unlabeled SynB1 and SynB3 did not significantly increase plasma membrane permeability (>90% of the cell population retained calcein). In contrast, the SynB5 and pAntp-(43–58) peptides at 40 μM started inducing the cell-lysis (Fig. 2*A*). The amount of internalized SynB peptides increased linearly with concentration (Fig. 2*B*), implying the absence of saturation in their cellular accumulation. Both the L- and D-forms of SynB1 and SynB3 showed similar behavior. At low concentrations, we observed a higher level of internalization of pAntp-(43–58) and SynB5 than SynB1 and SynB3. However, the lytic activity of SynB5 and pAntp-(43–58) at concentrations above 12 μM and 30 μM, respectively, prevented an investigation of the full range of concentrations for these peptides.

Peptide Localization—To confirm that all peptides were inside the cell, we examined their uptake and intracellular localization by confocal microscopy. Because the NBD probe exhibited a strong photo-bleaching during observation, the cells were incubated with peptides coupled to the more photostable fluorophore, TAMRA. As reported in Fig. 3, for each peptide we observed an intracellular punctuate pattern of fluorescence in the perinuclear region, suggesting that they are sequestered within endocytotic vesicles.

Metabolic Inhibitors—The influence of temperature and metabolic inhibitors on the intracellular accumulation of the SynB and pAntp-(43–58) peptides was studied to see whether the uptake depended on a translocation mechanism or a cellular process. We incubated NBD-SynB3 (6 μM) or NBD-pAntp-(43–58) (1 μM) with K562 cells at both 37 °C (with and without ATP-depletion) and 4 °C. As illustrated in Fig. 4*A*, the amounts of internalized SynB3 and pAntp-(43–58) at the low temperature corresponded to only 12.8 ± 0.7% and 7.6 ± 2.4% (± S.D.) of the control level, respectively. When the cells were energy-deprived by pre-incubation at 37 °C in a medium containing 0,1% sodium azide and 50 mM 2-deoxy-D-glucose (resulting in >80% reduction in cellular ATP), a marked decrease in the extent of internalization was observed for both SynB3 and pAntp-(43–58) (13.9 ± 1% and 17.4 ± 1.6% of the control level, respectively). Subsequent observation by confocal microscopy indicated that no detectable peptide was present inside the cells, which are in agreement with the quantitative flow cytometry measurements (Fig. 4*B*). As controls, the influence of low temperature and ATP depletion on the cell uptake of transferrin and Lucifer Yellow was examined. The former is internalized into K562 cells via receptor-mediated clathrin-dependent endocytosis (33), whereas the latter is known to enter into eukaryotic cells via fluid-phase endocytosis (34). Upon incubation of the cells with Tf (25 μg·ml^{-1}) or LY (1 mg·ml^{-1}) for 30 and 90 min, respectively, we observed localization in endocytotic vesicles as indicated by the granular pattern of fluorescence (Fig. 4*B*). Moreover, microscopy experiments indicated that the internalization of Tf was apparently abolished at 4 °C and in the absence of ATP, whereas quantitative measurements indicated that cell-associated Tf was reduced 2- and 5-fold, respectively (Fig. 4). The residual cell-associated fluorescence likely corresponds to the fraction of Tf bound to receptors at the cell surface (33). Similarly, the amount of internalized LY at the low temperature or in energy-deprived cells corresponded to 13.7 ± 2.4 and 21.6 ± 1.5%, respectively, of the levels measured at 37 °C. Additional assays indicated that the cell uptake of SynB1 and SynB5 was also abolished at low temperature or in ATP-depleted cells (Table II). Thus, the comparison of data obtained with CPPs, Tf, and LY strongly suggests that the cell uptake of CPPs is driven by an energy-dependent, temperature-sensitive process.

Translocation Behavior of pAntp-(43–58) in Lipid Vesicles—The results above suggest that the passive translocation of pAntp-(43–58) through the lipid matrix of plasma membranes does not represent the major mechanism of cell uptake. Using a protocol to detect a pore formation-translocation mechanism, we have shown previously that the Antennapedia homeodomain-derived peptide is unable to cross a non-cellular lipid bilayer (26). However, this peptide has been reported to diffuse inside lipidic vesicles without involving pore constitution (35). To shed light on this apparent contradiction, we have further investigated whether this peptide could diffuse through a lipid bilayer. For this purpose, we have applied a protocol previously used to demonstrate the translocation of the NBD-labeled

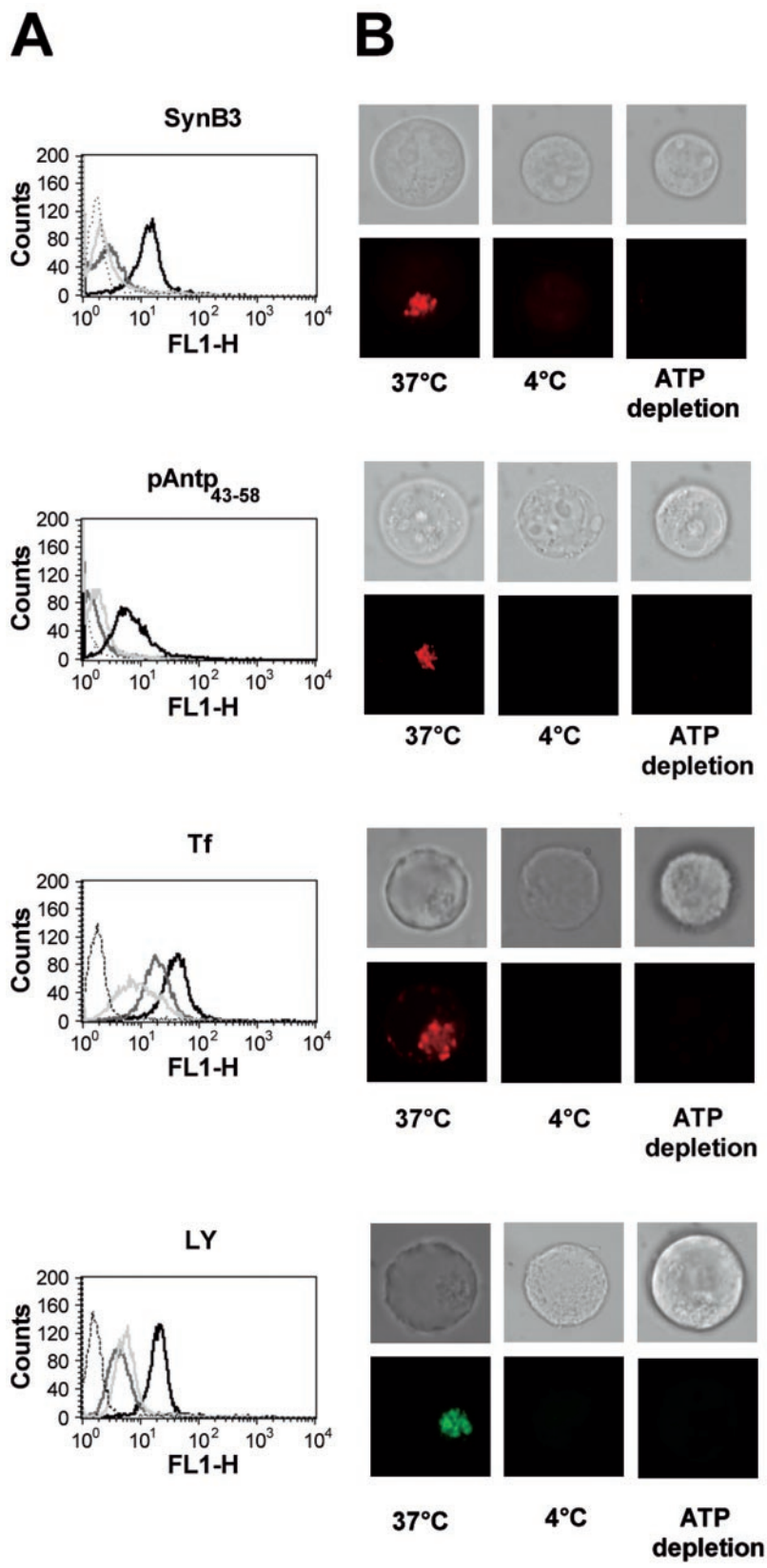

FIG. 4. **Influence of low temperature and ATP depletion on the cell uptake of SynB3, pAntp-(43–58), Tf, and LY.** *A*, flow cytometry analysis of the cell uptake of peptides and endocytosis markers. NBD-labeled SynB3 (at 6 μM for 90 min), NBD-labeled pAntp-(43–58) (1 μM for 90 min), FITC-Tf (25 $\mu g \cdot ml^{-1}$ for 30 min), or LY (1 $mg \cdot ml^{-1}$ for 90 min) in Opti-MEM were each incubated with K562 cells (6×10^5 $cells \cdot ml^{-1}$) at 37 °C or 4 °C or with energy-deprived K562 cells (see "Experimental Procedures"). Thereafter, the cells were washed twice in ice-cold PBS and analyzed by flow cytometry. For the SynB3 and pAntp-(43–58) peptides, the washed cells were treated for 5 min with dithionite prior to analysis. Legend of histograms as follows: *black lines*, experiments at 37 °C; *dark gray lines*, experiments at 4 °C; *gray lines*, experiments in ATP-depleted cells; and *dashed lines*, experiments with cells alone. *B*, confocal microscopy. TAMRA-SynB3 (90 min at 3 μM), TAMRA-pAntp-(43–58) (90 min at 1 μM), Texas-Red Tf (30 min at 25 $\mu g \cdot ml^{-1}$), or LY (1 $mg \cdot ml^{-1}$ for 90 min) were each incubated with K562 cells (6×10^5 $cells \cdot ml^{-1}$) in Opti-MEM at 37 °C or 4 °C or with energy-deprived K562 cells. Thereafter, the uptake was stopped by washing cells twice with ice-cold PBS (final volume of 50 μl). To observe the localization of Tf or LY, the cells were plated on poly-L-lysine coated slides, fixed, washed twice, and mounted. For peptides, the cells were observed unfixed. The optical sections presented here were localized approximately at the mid-height level of cells. Photos obtained by transmitted light microscopy indicate the contours of cells.

CoxIV presequence (MLSLRQSIRFFKPATRTLCSSRYLL) in phospholipid vesicles exhibiting a membrane potential (negative inside). As observed for this latter peptide, the presence of a membrane potential is not required for the diffusion step but, if present, could alter the distribution of cationic peptides across the membrane and allow the trapping of translocated peptides inside the vesicles (36). NBD-pAntp-(43–58) was incubated for different times with lipid vesicles at a lipid-to-peptide molar ratio, ensuring complete membrane-binding (data not shown) prior to adding either dithionite or trypsin. Even after a 10-min incubation, the peptide fluorescence was completely quenched by the dithionite, indicating that it re-

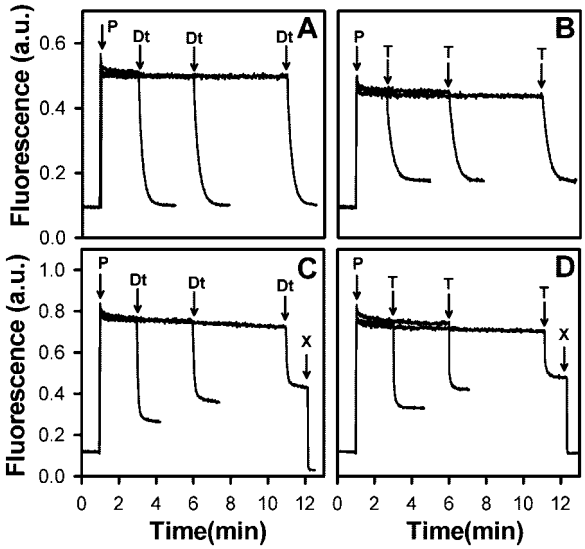

FIG. 5. **Measure of translocation of NBD-labeled pAntp-(43–58) and CoxIV peptides in phospholipid vesicles.** A stock of large unilamellar vesicles POPC/POPG (3:1; mol/mol) was diluted 100-fold in a buffer of 20 mM Hepes and 100 mM NaCl, pH 7 at 25 °C (final concentration of 164.5 μM) to create a membrane potential (see "Experimental Procedures"). After 1 min, the NBD-labeled peptide (*P*) (final concentration of 20 nM) was added to vesicles as indicated by the *arrow*. After various incubation times, the peptide-associated vesicles were treated either with 1 mM dithionite (*Dt*) or 30 μg·ml^{-1} trypsin (*T*) as indicated by the *arrows*. *A* and *B*, pAntp-(43–58). *C* and *D*, CoxIV presequence. For the latter, the addition of Triton X-100 (*X*) renders the peptide accessible to dithionite or trypsin. Each figure contains superposed traces representative of several experiments.

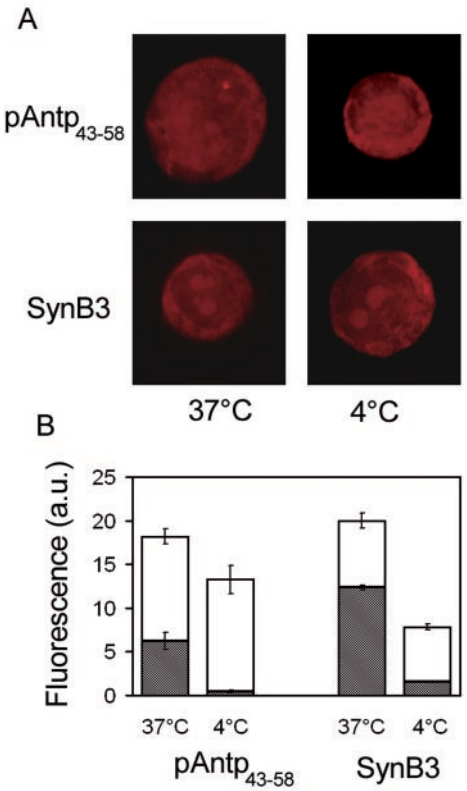

FIG. 6. **Intracellular localization of pAntp-(43–58) and SynB3 peptides in fixed cells.** *A*, K562 cells (6×10^5 cells·ml^{-1}) were incubated with either TAMRA-pAntp-(43–58) (1 μM) or TAMRA-SynB3 (3 μM) for 90 min at 37 °C or 4 °C. To observe the intracellular localization of peptide in fixed cells, the cells were washed twice in cold-PBS, plated on poly-L-lysine-coated slides for 45 min at 4 °C, fixed with 3.7% formalin (in PBS) for 10 min, washed twice with ice-cold PBS, dried, and mounted. *B*, K562 cells (6×10^5 cells·ml^{-1}) were incubated with NBD-pAntp-(43–58) and NBD-SynB3 in Opti-MEM for 90 min at either 37 °C or 4 °C. The amount of cell-associated and internalized peptide was determined by the NBD/dithionite assay (see "Experimental Procedures"). The amount of peptide bound to the cell surface (*open bar*) was obtained by subtracting the amount of internalized peptide (*closed bar*) from the amount of cell-associated peptide. Each point is the mean ± S.D. of three separate determinations.

mained bound to the outer leaflet of the lipid vesicles as shown in Fig. 5*A*. In addition, trypsin treatment resulted in a similar decrease of fluorescence, confirming that the fluorescent peptide was indeed externally accessible to the enzyme (Fig. 5*B*). In contrast, a significant fraction of the NBD-CoxIV peptide was progressively protected from dithionite or trypsin treatment in a time-dependent manner (Fig. 5, *C* and *D*), which is in agreement with other published results (36). These results confirm that pAntp-(43–58) is unable to diffuse across noncellular lipid bilayers.

Effect of Cell Fixation on the Uptake of pAntp-(43–58) and SynB Peptides—Recently, it has been reported that various cell fixation protocols induce the apparent translocation and nucleolar localization of the positively charged DNA-binding or Tat-fusion proteins (37, 38) and the Tat-(48–60) peptide (39). We have examined the possibility that the temperature-independent translocation of pAntp-(43–58), commonly observed in fixed cells (4, 20, 40), could be the result of such an effect. As shown in Fig. 6*A*, fixation of K562 cells, incubated with 1 μM TAMRA-pAntp-(43–58) for 90 min at 37 °C and washed twice, resulted in a fluorescence localization in the cytoplasm and nucleus that was not observed in unfixed cells (by comparison to Fig. 3). Identical results were obtained by incubating the cells with peptides at 4 °C. This observation was not restricted to pAntp-(43–58), because we obtained similar results with 3 μM TAMRA-SynB3 (Fig. 6) and other SynB peptides (data not shown). In Fig. 6*B*, we show that a significant fraction of NBD-pAntp-(43–58) and NBD-SynB3, incubated at 4 °C, was present on the surface of washed cells. This supports the interpretation that, after low temperature incubation and cell washing, a large proportion of surface-bound peptide diffuses into the cytoplasm during the fixation step (37).

Internalization in the Presence of Endocytosis Inhibitors—To further explore the possibility that CPPs enter into the cells by an endocytotic mechanism, we looked at the effect of endocytosis inhibitors on their intracellular accumulation and localization. As shown in Fig. 7*A*, treatment of cells for 1 h with microtubule-disrupting reagents such as vinblastine (10 μM) or nocodazole (20 μM) (41, 42), prior to the addition of SynB3, resulted in a diminution of the amount of internalized peptide (59.6 ± 2.6 and 63.2 ± 5.1%, respectively, of the control level). Moreover, we observed that both drugs strongly modified the repartition of TAMRA-SynB3-containing vesicles (Fig. 7*B*), retaining them close to the cell periphery rather than a largely perinuclear localization in the control cells. As expected, disruption of the microtubules altered the cellular distribution of LY-labeled vesicles in a similar manner (Fig. 7*C*). Because endocytosed fluid phase markers are conveyed from the peripheral to the perinuclear region via a microtubule-dependent transport process (41), our results suggest that SynB3 may follow the same pathway. In contrast, studies in which actin filaments were disassembled by a 1-h treatment with cytochalasin D (10 μM) showed no significant effect on either accumulation or localization of SynB3 (Fig. 7).

The role of intracellular pH on the internalization of CPPs was investigated using known neutralization agents. The weak base NH_4Cl (10 mM), known to neutralize the acidification of endosomal and lysosomal compartments, caused a reduction in the cell uptake of SynB3 (Fig. 7*A*). Control experiments (data not shown) suggested that the luminal pH of endosomes was

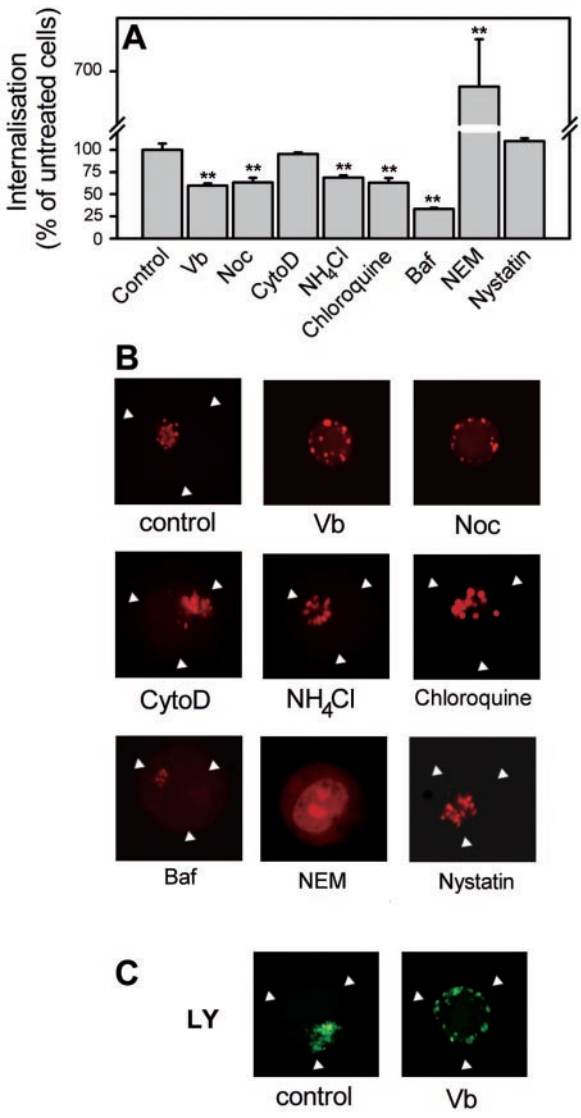

FIG. 7. **Influence of various endocytosis inhibitors on the cell uptake of SynB3.** *A*, for flow cytometry analysis, K562 cells (6×10^5 cells·ml^{-1}) were incubated with NBD-labeled SynB3 peptide at 6 μM for 90 min at Opti-MEM. The cells were treated with the different inhibitors as detailed under "Experimental Procedures." The extent of cell uptake was determined by the NBD/dithionite assay. For each experiment, the mean fluorescence intensity measured with the cells alone was subtracted from the mean fluorescence intensity measured with the peptide. The values were normalized to that of the control experiment without inhibitors. Each point is the mean ± S.D. of three separate determinations. Statistical significance was assessed by analysis of variance (ANOVA), **, $p < 0.01$). *B*, K562 cells untreated or treated with inhibitors (see "Experimental Procedures") were incubated with TAMRA-SynB3 at 3 μM for 90 min in Opti-MEM at 37 °C. Thereafter, the cells were carefully washed twice with ice-cold PBS (final volume of 50 μl) and immediately observed by confocal fluorescence microscopy. *C*, LY-labeled vesicles. For *panels B* and *C*, the optical sections presented correspond approximately to the mid-height level of cells. *Arrowheads* indicate the contours of cells. *Vb*, vinblastine; *Noc*, nocodazole; *CytoD*, cytochalasin D; *Baf*, bafilomycin A1.

modified, because we observed a reduced uptake of Tf, the receptor-mediated recycling of which is pH-sensitive (33, 43). We also observed an inhibition of uptake of SynB3 in the presence of 50 μM chloroquine (acting also as a weak base) and a more pronounced inhibition by 200 nM bafilomycin A1 (Baf), which directly blocks endosome acidification by inhibiting the vacuolar (ATPase) proton pump (44). As reported previously, NH_4Cl and chloroquine are known to cause the swelling of endosomes and lysosomes (45, 46), which is consistent with our observation that SynB3 was located in enlarged vesicles after these treatments. Furthermore, in the presence of bafilomycin A1 the number of peptide-labeled vesicles was also highly reduced (Fig. 7*B*).

When cells were treated with NEM (10 μM), an endocytosis inhibitor reacting with −SH functions, the uptake of SynB3 was unexpectedly increased, whereas the internalization of Tf was abolished (data not shown). As shown by confocal microscopy, SynB3 in NEM-treated cells was not localized inside vesicles but was homogeneously distributed throughout the cytoplasm and in the nucleus (Fig. 7*B*).

We also looked at the uptake and localization of SynB3 in the presence of nystatin (1 h; 25 μg·ml^{-1}), a drug that complexes cholesterol and alters the structure and function of glycolipid microdomains and caveola (47). No effects were seen, suggesting that the internalization of SynB3 occurred by a caveola-independent pathway. Likewise, no diminution of the cell uptake of Tf and LY was observed in the presence of this inhibitor (data not shown).

To establish the generality of our observations with SynB3, the internalization behaviors of SynB1, SynB5, and pAntp-(43–58) in the presence of these various inhibitors were tested and found to be essentially identical to that of SynB3, as summarized in Table II. This was also confirmed by confocal microscopy (data not shown).

Finally, we examined whether the internalization of CPPs was dependent on interaction with the negatively charged plasma membrane by looking at peptide uptake in the presence or absence of 300 μM poly-L-lysine. The peptide concentrations (40 μM for SynB1 and SynB3, 1 μM for pAntp-(43–58), and 3 μM for SynB5) were chosen to ensure a sufficient occupancy of the cell-surface. As shown in Table II, poly-L-lysine strongly reduced internalization of all four peptides, implying a possible adsorptive role for the negatively charged membrane.

DISCUSSION

The objective of the studies described above was to better understand the mechanism of cell uptake of the SynB series of CPPs and that of pAntp-(43–58). We sought to achieve this by combining flow cytometry (30), an essentially quantitative method that allows accurate measurement of peptide internalization, with confocal microscopy. First, we showed that the CPPs in this study rapidly enter into K562 cells at low micromolar concentrations, confirming the results obtained previously with pAntp-(43–58), SynB1, and SynB5 (27, 30). The fact that the D-enantiomer forms of SynB1 and SynB3 accumulated in K562 cells suggests that these vectors do not require a stereospecific receptor to reach the cell interior, which is consistent with previous studies on pAntp-(43–58) or MAP (8, 20). The cell uptake of all peptides depended linearly on the extracellular concentration up to 40 μM. The absence of a saturating effect within this concentration range has also been seen with other CPPs (8, 20, 48). The variation in uptake efficiency (compare SynB1/3/5 and pAntp-(43–58) in Fig. 2) may be related to the slightly different charge and/or hydrophobicity properties expected to influence the cell-penetrating activity of cationic peptides (30). Of particular note was the observation that SynB1 and SynB3 have no significant lytic activity even at high concentrations, whereas increasing concentrations of SynB5 and pAntp-(43–58) perturbed the integrity of the plasma membrane. By assessing the cellular distribution of the CPPs by confocal microscopy, we have observed their strong association with vesicular structures, suggesting an endocytotic process. To explore this mechanism further, we first determined the influence of low temperature and metabolic inhibition on the cellular uptake of SynB and pAntp-(43–58) peptides. We observed that the intracellular accumulation of these peptides is

TABLE II
Effect of metabolic and endocytosis inhibitors on the uptake of CPPs

Inhibitors (concentration)	Cell uptake of peptide[a]			
	SynB1[b]	SynB3	SynB5	PAntp-(43–58)
	% untreated control ± S.D.			
37 °C (control)	100 ± 1.8	100 ± 1.9	100 ± 6.5	100 ± 15.7
4 °C	10.8 ± 3.9**	12.8 ± 0.7**	2.4 ± 0.8**	7.6 ± 2.4**
NaN_3(0.1%) + DOG (50 mM)	12.4 ± 3.1**	13.9 ± 1**	10.3 ± 1.9**	17.4 ± 1.6**
Vinblastine (10 μM)	62.3 ± 7.6*	59.6 ± 2.6**	27.9 ± 0.5**	66.8 ± 2.3*
Nocodazole (20 μM)	77.1 ± 0.2**	63.2 ± 5.1**	36.6 ± 2.5**	86.1 ± 6.2
Cytochalasin D (10 μM)	76.5 ± 2.9*	95.9 ± 1.7	93.8 ± 2.3	75 ± 6.9
NEM (10 μM)	330.1 ± 9.3**	685.6 ± 44.6**	220.5 ± 10.5**	95.8 ± 8.4
NH_4Cl (10 mM)	49.7 ± 1.4**	68.6 ± 2.6**	39.5 ± 1.2**	55.4 ± 4.4**
Chloroquine (50 μM)	55.1 ± 1.5**	64.9 ± 4.4**	66.9 ± 1.1**	69.4 ± 3.9**
Bafilomycin A1 (200 nM)	32.3 ± 4.9**	33.3 ± 1.32**	38.3 ± 4.7**	26.9 ± 4.1**
Nystatin (25 $\mu g \cdot ml^{-1}$)	93 ± 3.3*	109.8 ± 3.3	85.3 ± 13.4	85.2 ± 1.6**
Poly-L-lysine (300 μM)[c]	37.5 ± 4.5**	51.2 ± 1.6**	46.3 ± 8.3**	62.7 ± 2.2**

[a] The cells were treated with inhibitors as described under "Experimental Procedures." For each experiment, the mean fluorescence intensity measured with the cells alone was subtracted from the mean fluorescence intensity measured with the peptide. Each value was therefore normalized to the value obtained with the untreated cells incubated with peptide at 37 °C (control experiments). Each value is the mean ± S.D. of three separate determinations. Statistical significance was assessed by analysis of variance (*, $p < 0.05$; **, $p < 0.01$).

[b] NBD-SynB1 and NBD-SynB3 were incubated at 6 μM, NBD-SynB5 was incubated at 3 μM, and NBD-pAntp-(43–58) at 1 μM for 90 min with K562 cells (6×10^5 cells·ml^{-1}) in Opti-MEM.

[c] Inhibition assays with poly-L-lysine were performed with 40 μM NBD-SynB1, 40 μM NBD-SynB3, 3 μM NBD-SynB5, and 1 μM NBD-pAntp-(43–58) incubated with cells for 15 min.

abolished at low temperature or in ATP-deprived cells. In parallel, we showed that, under the same experimental conditions, receptor-mediated and fluid-phase endocytotic pathways were also inhibited, consistent with previous reports (33, 34, 43, 49). These results provide strong evidence that the uptake of the CPPs depends on a cellular process related to endocytosis rather than a translocation mechanism. This observation corroborates our previous data suggesting that SynB peptides, derived from PG-1 linearization, are unable to spontaneously cross a lipid membrane (27). Likewise, this is consistent with our results indicating that pAntp-(43–58) peptide was unable to pass across a non-cellular phospholipid bilayer either by a translocation-pore formation process (26) or diffusion as reported here.

We cannot confirm previous studies on the temperature-independent cellular uptake of pAntp-(43–58) that were carried out using indirect fluorescent microscopy (4, 20, 40). Studies similar to our own have suggested that the fixation of cells, used in the microscopy experiments, induces the cytoplasmic and nuclear accumulation of several cationic proteins (37, 38). A more recent study has also shown that Tat-(48–60) does not enter into live cells at low temperature (39), contrary to earlier observations carried out in fixed cells (5). Our own experiments have demonstrated that the fixation of K562 cells induces the entry of the Antennapedia homeodomain-derived peptide and the SynB peptides in a temperature-independent manner and alters their intracellular localization. A possible origin of this artifact, suggested by Lundberg and Johansson (37), is that the cationic peptides or proteins interact with the plasma membrane at a low temperature, remain attached to the cell surface during the washing steps, and then diffuse inside the cells during the fixation step. Supporting this view, our experiments indicate that a fraction of peptides remains bound to the cell surface after incubation at 4 °C followed by a washing step.

Thus, our results suggest that the cell-penetrating activity of cationic peptides could be unrelated to a temperature-independent mechanism. However, we cannot rule out the possibility that a non-endocytotic mechanism contributes, at a low level, to the internalization of particular CPPs. Oekhle *et al.* (8), using a method analogous to the NBD/dithionite assay, determined that MAP enters partially into cells by an energy- and temperature-independent mechanism. To analyze these results, they suggested that MAP penetrates across the lipidic area of the plasma membrane (8). Likewise, Takeshima *et al.* (50) reported recently that analogues of magainin 2 and buforin, which have been demonstrated to translocate into liposomal systems, could enter into eucaryotic cells in a non-endocytic manner.

Further mechanistic insights were provided by an examination of the influence of endocytosis inhibitors on the internalization of the CPPs. In control cells, the vesicular accumulation of peptides and LY resulted in fluorescence staining in the perinuclear region, characteristic of late endosomes and lysosomes (51). In the presence of microtubule-disrupting reagents, the cellular accumulation of peptides was reduced and, as was found with LY, peptides remained inside vesicles localized to the cell periphery rather than the perinuclear region. It is generally accepted that substrates entering by constitutive fluid phase endocytosis are routed from the early endosomes to the late endosomes and lysosomes (51–53) via endosomal carrier vesicles (ECVs). In addition, as observed in K562 cells, it has been established that this transport is dependent on an intact microtubule network (41, 51). Our results therefore suggest that CPPs and LY, once internalized, follow an identical endocytotic pathway toward late endosomes and lysosomes. This agrees well with our kinetic data suggesting that the L-peptides may be degraded within a lysosomal compartment.

Further support for this localization comes from experiments wherein a marked change in the morphology of fluorescently labeled vesicles is seen when cells are treated either with NH_4Cl or chloroquine, confirming that the peptides are within an acidic compartment. In addition, these two treatments inhibited peptide accumulation into the cells as measured by flow cytometry. Because the formation of endosome carrier vesicles is dependent on the acidification of their luminal interiors, it is likely that the neutralization of the endosomal pH blocks the transfer of peptide to late endosomes, as was observed elsewhere for fluid-phase markers (44, 54). Experiments with bafilomycin A1 support this proposal, because this specific inhibitor of the vacuolar ATPase, which is more effective than NH_4Cl in preventing acidification of early endosomes and the formation of endosomal carrier vesicles (44), produces a more marked inhibition of peptide internalization.

Surprisingly, we observed that NEM enhances the apparent uptake of CPPs while inhibiting the internalization of Tf in K562 cells (data not shown, but see Ref. 55). However, microscopy experiments revealed that, in NEM-treated cells, the pep-

tides are not associated with vesicular structures but rather are homogeneously distributed throughout the cytoplasm and nucleus. Considering that the fluorescence of the NBD peptide could be partially self-quenched because of its concentration into vesicles, it is likely that the observed higher fluorescence intensity could reflect its diffusion in the entire cells. Our results indicate that NEM does not influence the entry of CPPs but strongly affects their transport along the endosomal pathway. Previously, Oekhle *et al.* (8) quantified the NEM-induced inhibition of MAP degradation in endothelial cells but did not study its intracellular localization. It is probable that disruption of the endocytotic transport followed by the CPPs could prevent their access to a degradation compartment.

Upon examination of the involvement of caveolae in CPPs uptake, we have shown that nystatin has no effect on the cellular uptake of CPPs. This drug did not markedly modify the cell uptake of SynB peptides or that of LY and did not affect the clathrin-mediated endocytosis of Tf, as expected (56).

Finally, treatment of cells with the actin-disrupting reagent cytochalasin D did not modify the internalization of peptides. This is in accord with other recent results showing that the actin cytoskeleton may not play a major role in endocytotic processes in K562 cells (42, 57).

As suggested above, certain physico-chemical properties (positive charge, hydrophobicity, and amphipathicity) may govern the cell-penetrating ability of this class of peptides. However, because many different peptide sequences enter by a common endocytotic pathway, this suggests that such properties *per se* do not confer specific translocating features but may instead govern their adsorptive affinity for a cell surface. Consistent with this view, we show that the polycation poly-L-lysine acts as a competitive inhibitor of cell uptake. Again, it has been reported that the positive charge of peptides such as Tat-(48–60) mediates an interaction with proteoglycans (6). However, for pAntp-(43–58) (21, 26) or SynB5 (27) it is likely that the lipid-binding ability (related to their hydrophobicity and amphipathicity) also contributes to their affinity for cell membranes. This type of lipid interaction may be responsible for their ability to destabilize plasma membrane at high concentrations, leading to cell lysis as was found for pAntp-(43–58), MAP, and Transportan (19, 48). In contrast, the highly polar peptides Tat-(48–60) (5, 18, 48), SynB1, and SynB3, although showing a reduced uptake compared with the more hydrophobic classes of CPP, do not induce cell permeabilization, suggesting that their interaction with the plasma membranes is not destabilizing in nature. Because of their low cytotoxicity, SynB1 and SynB3 peptides represent valuable CPPs for therapeutic applications, as confirmed by several *in vivo* studies (15–17).

In conclusion, our results suggest that protegrin- and Antennapedia homeodomain-derived cell-penetrating peptides enter via a common adsorptive-mediated endocytosis pathway rather than a translocation mechanism. In particular, these results agree well with *in vivo* studies indicating that a similar mechanism operates in capillary endothelial cells during the passage of SynB1 and SynB3 across the blood-brain barrier (58). In the future, we anticipate that CPPs of the type we have described here will be used routinely in therapeutic applications in which the release of drugs from endosomal and lysosomal compartments in target cells is of critical importance.

Acknowledgments—We acknowledge Dr. F. Roux and the Synt:em production team for peptide synthesis and purification. Imaging was performed at the Integrated Imaging Facility of IFR24 (Montpellier). We thank Dr. P. Travo, head of the Facility, for constant interest and support.

REFERENCES

1. Lindgren, M., Hällbrink, M., Prochiantz, A., and Langel, U. (2000) *Trends Pharmacol. Sci.* **21,** 99–103
2. Dunican, D. J., and Doherty, P. (2001) *Biopolymers* **60,** 45–60
3. Schwarze, S. R., Hruska, K. A., and Dowdy, S. F. (2000) *Trends Cell Biol.* **10,** 290–295
4. Derossi, D., Joliot, A. H., Chassaing, G., and Prochiantz, A. (1994) *J. Biol. Chem.* **269,** 10444–10450
5. Vivès, E., Brodin, P., and Lebleu, B. (1997) *J. Biol. Chem.* **272,** 16010–16077
6. Futaki, S., Suzuki, T., Ohashi, W., Yagami, T., Tanaka, S., Ueda, K., and Sugiura, Y. (2001) *J. Biol. Chem.* **276,** 5836–5840
7. Pooga, M., Hällbrink, M., Zorko, M., and Langel, U. (1998) *FASEB J.* **12,** 67–77
8. Oehlke, J., Scheller, A., Wiesner, B., Krause, E., Beyermann, M., Klauschenz, E., Melzig, M., and Bienert, M. (1998) *Biochim. Biophys. Acta* **1414,** 127–139
9. Chaloin, L., Vidal, P., Heitz, A., Van Mau, N., Méry, J., Divita, G., and Heitz, F. (1997) *Biochemistry* **36,** 11179–11187
10. Vidal, P., Chaloin, L., Heitz, A., Van Mau, N., Méry, J., Divita, G., and Heitz F. (1998) *J. Membr. Biol.* **162,** 259–264
11. Kokryakov, V. N., Harwig, S. S., Panyutich, E. A., Shevchenko, A. A., Aleshina, G. M., Shamova, O. V., Korneva, H. A., and Lehrer, R. I. (1993) *FEBS Lett.* **327,** 231–236
12. Aumelas, A., Mangoni, M., Roumestand, C., Chiche, L., Despaux, E., Grassy, G., Calas, B., and Chavanieu, A. (1996) *Eur. J. Biochem.* **237,** 575–583
13. Mangoni, M. E., Aumelas, A., Charnet, P., Roumestand, C., Chiche, L., Despaux, E., Grassy, G., Calas, B., and Chavanieu A. (1996) *FEBS Lett.* **383,** 93–98
14. Sokolov, Y., Mirzabekov, T., Martin, D., Lehrer, R. I., and Kagan, B. L. (1999) *Biochim. Biophys. Acta* **1420,** 23–29
15. Rousselle, C., Clair, P., Lefauconnier, J. M., Kaczorek, M., Scherrmann, J. M., and Temsamani, J. (2000) *Mol. Pharmacol.* **57,** 679–686
16. Rousselle, C., Clair, P., Temsamani, J., and Scherrmann, J. M. (2002) *J. Drug Target.* **10,** 309–315
17. Mazel, M., Clair, P., Rousselle, C., Vidal, P., Scherrmann, J. M., Mathieu, D., and Temsamani, J. (2001) *Anticancer Drugs* **12,** 107–116
18. Suzuki, T., Futaki, S., Niwa, M., Tanaka, S., Ueda, K., and Sugiura, Y. (2002) *J. Biol. Chem.* **277,** 2437–2443
19. Scheller, A., Oehlke, J., Wiesner, B., Dathe, M., Krause, E., Beyermann, M., Melzig, M., and Bienert M. (1999) *J. Pept. Sci.* **5,** 185–194
20. Derossi, D., Calvet S., Trembleau A., Brunissen A., Chassaing G., and Prochiantz, A. (1996) *J. Biol. Chem.* **271,** 18188–18193
21. Berlose, J. P., Convert, O., Derossi, D., Brunissen, A., and Chassaing, G. (1996) *Eur. J. Biochem.* **242,** 372–386
22. Dathe, M., Schümann, M., Wieprecht, T., Winkler, A., Beyermann, M., Krause, E., Matsuzaki, K., Murase, O., and Bienert, M. (1996) *Biochemistry* **35,** 12612–12622
23. Lindberg, M., Jarvet, J., Langel, U., and Gräslund, A. (2001) *Biochemistry* **40,** 3141–3149
24. Magzoub, M., Kilk, K., Eriksson, L. E., Langel, U., and Gräslund, A. (2001) *Biochim. Biophys. Acta* **1512,** 77–89
25. Matsuzaki K. (1999) *Biochim. Biophys. Acta* **1462,** 1–10
26. Drin, G., Déméné, H., Temsamani, J., and Brasseur, R. (2001) *Biochemistry* **40,** 1824–1834
27. Drin, G., and Temsamani, J. (2002) *Biochim. Biophys. Acta* **1559,** 160–170
28. Bartlett, G. R. (1959) *J. Biol. Chem.* **234,** 466–468
29. Sims, P. J., Waggoner, A. S., Wang, C., and Hoffma, J. F. (1974) *Biochemistry* **13,** 3315–3330
30. Drin, G., Mazel, M., Clair, P., Mathieu, D., Kaczorek, M., and Temsamani, J. (2001) *Eur. J. Biochem.* **268,** 1304–1314
31. Eisenberg, D., Weiss, R. M., and Terwilliger, T. C. (1982) *Nature* **299,** 371–374
32. Fauchére, J. L., and Pliska, V. E. (1983) *Eur. J. Med. Chem.* **18,** 369–375
33. Klausner, R. D., Van Renswoude, J., Ashwell, G., Kempf, C., Schechter, A. N., Dean, A., and Bridges, K. R. (1983) *J. Biol. Chem.* **258,** 4715–4724
34. Swanson, J. (1989) in *Fluorescence Microscopy of Living Cells in Culture* (Wang, Y. L., and Taylor, D. L., eds), pp. 137–151, Academic Press, New York
35. Thorén, P. E. G, Persson, D., Karlsson, M., and Nordén, B. (2000) *FEBS Lett.* **482,** 265–268
36. Maduke, M., and Roise, D (1993) *Science* **260,** 364–367
37. Lundberg, M., and Johansson, M. (2002) *Biochem. Biophys. Res. Commun.* **291,** 367–371
38. Leifert, J. A., Harkins, S., and Whitton J. L. (2002) *Gene Ther.* **9,** 1422–1428
39. Richard, J. P., Melikov, K., Vivès, E., Ramos, C., Verbeure, B., Gait, M. J., Chernomordik, L. V., and Lebleu, B. (2003) *J. Biol. Chem.* **278,** 585–590
40. Lindgren, M., Gallet, X., Soomets, U., Hällbrink, M., Bråkenhielm, E., Pooga, M., Brasseur, R., and Langel U. (2000) *Bioconjug. Chem.* **11,** 619–626
41. Jin, M., and Snider, M. D. (1993) *J. Biol. Chem.* **268,** 18390–18397
42. Thatte, H. S., Bridges, K. R., and Golan, D. E. (1994) *J. Cell. Physiol.* **160,** 345–357
43. Breuer, W., Epsztejn, S., and Cabantchik, Z. I. (1995) *J. Biol. Chem.* **270,** 24209–24215
44. Clague, M., Urbé, S., Aniento, F., and Gruenberg, J. (1994) *J. Biol. Chem.* **269,** 21–24
45. Brown, W. J., Constantinescu, E., and Farquhar, M. G. (1984) *J. Cell Biol.* **99,** 320–326
46. Brown, W. J., Goodhouse, J., and Farquhar, M. G. (1986) *J. Cell Biol.* **103,** 1235–1247
47. Anderson, R. G., Kamen, B. A., Rothberg, K. G., and Lacey, S. W. (1992) *Science* **255,** 410–411
48. Hällbrink, M., Florén, A., Elmquist, A., Pooga, M., Bartfai, T., and Langel, U. (2001) *Biochim. Biophys. Acta* **1515,** 101–109
49. Schmidt, S. L., and Carter, L. L. (1990) *J. Cell Biol.* **111,** 2307–2318
50. Takeshima, K., Chikushi, A., Lee, K., Yonehara, S., and Matsuzaki, K. (2003)

J. Biol. Chem. **278,** 1310–1315
51. Gruenberg, J., Griffiths, G., and Howell, K. E. (1989) *J. Cell Biol.* **108,** 1301–1316
52. Gruenberg, J., and Maxfield, F. R. (1995) *Curr. Opin. Cell Biol.* **7,** 552–563
53. Pillay, C. S., Elliott, E., and Dennison, C. (2002) *Biochem. J.* **363,** 417–429
54. Bayer, N., Schober, D., Partal, E., Murphy, R. F., Blaas, D., and Fuchs, R. (1998) *J. Virol.* **72,** 9645–9655
55. Bérczi, A., Ruthner, M., Szüts, V., Fritzer, M., Schweinzer, E., and Goldenberg, H. (1993) *Eur. J. Biochem.* **213,** 427–436
56. Puri, V., Watanabe, R., Singh, R. D., Dominguez, M., Brown, J. C., Wheatley, C. L., Marks, D. L., and Pagano, R. E. (2001) *J. Cell Biol.* **154,** 535–547
57. Fujimoto, L. M., Roth, R., Heuser, J. E., and Schmid, S. L. (2000) *Traffic* **1,** 161–171
58. Rousselle, C., Smirnova, M., Clair, P., Lefauconnier, J. M., Chavanieu, A., Calas, B., Scherrmann, J. M., and Temsamani, J. (2001) *J. Pharmacol. Exp. Ther.* **296,** 124–131